CHAPTER 2

EXPERIMENTAL DETAILS

In this chapter we provide details of the methods used for preparation of different NPs (ORMOSIL NP [45, 97], gold nanorods [77, 98], polymeric NPs [99] and liposomes [100, 101]) used for the studies described in the thesis. The methods used to characterize these and to study their interaction with dyes are also detailed. Finally we describe the methodology used for determination of cellular toxicity due to dye-NP conjugates [102] and to calculate the molarity of the NPs.

For all the preparations and experiments, water from a Millipore Milli-Q system was used.

2.1 Synthesis of NPs

2.1.1 ORMOSIL NP (SiNP-V, SiNP-VA)

The ORMOSIL NPs were synthesized using microemulsion based sol-gel method, also called modified Stober's method [45]. For this the chemicals: silica precursors vinyl-triethoxysilane (VTES), 3-aminopropyl-triethoxysilane (APTS), surfactant dioctyl sodium sulfosuccinate (aerosol OT (AOT)), 1-Butanol (spectroscopic grade) were purchased from Sigma and used as received. The schematic diagram depicting combined microemulsion/sol-gel process for producing SiNPs is shown in Fig. 2.1. Two types of ORMOSIL NP, one with silica precursor vinyl-triethoxysilane (VTES) and other with both VTES and 3-aminopropyl-triethoxysilane (APTS) were synthesized.

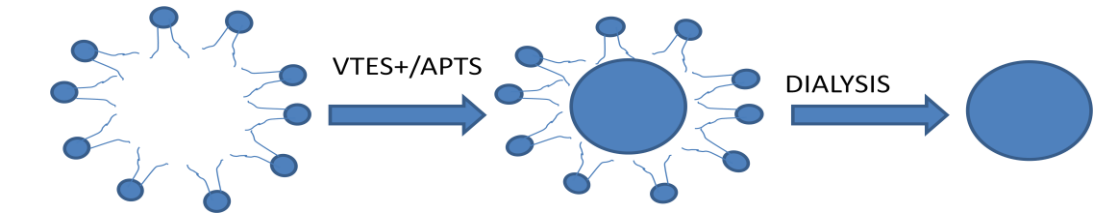

AOT/Butanol/water micelles

VTES+/APTS NP in AOT/Butanol/water micelles

VTES+/APTS NP Dispersed in Aqueous Medium

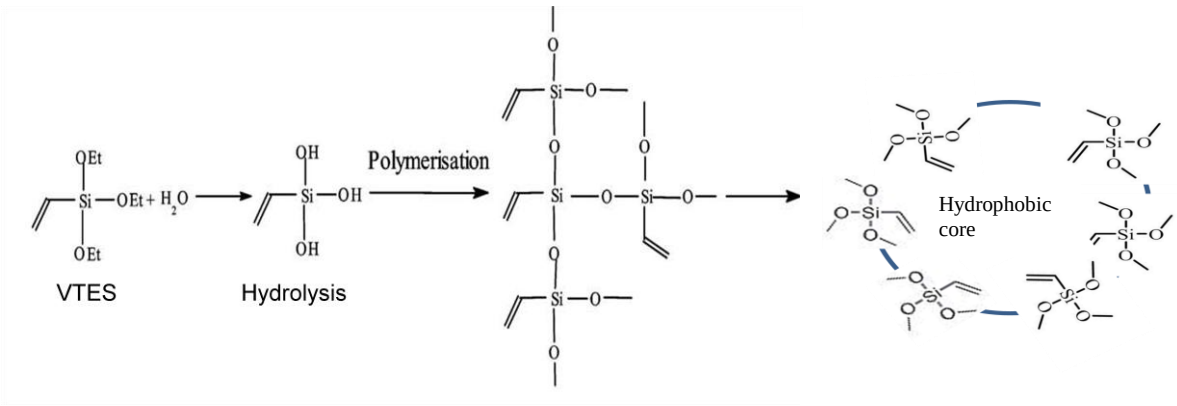

Figure 2.1 *The schematic diagram of combined microemulsion/sol-gel process for producing SiNPs. Recreated from ref. [51, 97]*

Amine modified SiNPs (SiNP-VA) were synthesized in the non polar core of anionic surfactant AOT (Mol. Wt. 444.56, cmc~1mM)/1-Butanol/water micellar system using VTES and APTS following the method as described in reference 45. In this method, first the micelles were prepared by dissolving 0.44g AOT and 800µl of 1-butanol (used as co-surfactant) in 20ml of water under vigorous magnetic stirring for ~ 1 h. VTES (200ul) was added to this micellar system. The resulting solution was stirred until it became visibly transparent. After ~30minutes, APTS (20 µL) was added to the solution, which was further stirred for about 20 h. The entire reaction was carried out at room temperature. At the end of the process, a bluish white translucency, indicating the formation of nanoparticles, was observed. NPs with only VTES silica precursor (SiNP-V)

were prepared following the same procedure. However in place of APTS, 20 μL of aqueous ammonia (30 %) was added as the reducing agent. The SiNPs were purified from AOT and butanol by dialyzing (using a membrane having a molecular cut-off 10 kDa) against neutral water for a period of ~96 hours such that the SiNP colloidal suspension did not show the standing froth due to the presence of AOT after dialysis. These SiNPs were kept at 10 degree centigrade till use and were found to be stable for more than a year.

2.1.2 Gold Nanorods

CTAB-coated AuNRs having different L-SPR were synthesized, by Dr. A.Uppal and Dr. R.Shrivastava, following the seed mediated growth procedure [77, 98]. The chemicals used : $HAuCl_4 \cdot 3H_2O$, CTAB, l-ascorbic acid, $NaBH_4$, $AgNO_3$, polymers polystyrene sulphonate (PSS), poly allylamine hydrochloride (PAH) and poly diallyl dimethyl ammonium chloride (PDDAC) were purchased from Sigma-Aldrich and were used as received.

First, CTAB capped seeds were prepared by chemical reduction of $HAuCl_4$ with sodium borohydride. For this 5 ml of 0.2 M CTAB was mixed with 5 ml of 5 mM $HAuCl_4$. Then 0.6 ml of ice cold 0.01 M $NaBH_4$ was added while stirring for 2 minutes. The seed solution was kept at room temperature and used within 2-5 hours. For synthesis of AuNRs having L-SP around ~660 nm, the growth solution containing 10 ml of 0.2 M CTAB, 10 ml of 1 mM $HAuCl_4$, 120 μl of 0.01M $AgNO_3$ and 144 μl of 0.1 M ascorbic acid was prepared. After that, 24 μl of seed solution was added to the growth solution to initiate the growth of the AuNRs. For AuNRs having L-SP around ~800 nm the growth solution was prepared by mixing 8 ml of 2 mM $HAuCl_4$, 12.6 ml water, 19 ml of 0.2 M CTAB, 160 μl of 0.015 M $AgNO_3$ and 256 μl of 0.1 M ascorbic acid. After that 175 μl of seed solution was added to initiate the growth of the AuNRs.

Coating of AuNRs with polymers PSS, PAH and PDDAC:

As CTAB coated rods were positively charged, these were first coated with negatively charged polymer PSS and then coated with positively charged polymers PAH or PDDAC. For this AuNR solution was centrifuged at 10,000 rpm for 30 minutes and then the sediment was re-suspended in Millipore water to remove the extra CTAB. This procedure was repeated once more and then the rods were suspended in 1 mM sodium chloride solution containing 2 mg/mL PSS. The nanorod solution was stirred for 2-3 hours and then centrifuged at 12,000 rpm. The attachment of PSS onto the AuNR surface was confirmed by checking the zeta potential of the AuNRs (as described in section 2.2.3). The sediment was then re-suspended into a 3 mg/ml PDDAC or PAH solution in 1mM sodium chloride, stirred for 2-3 hours and then centrifuged twice at 12,000 rpm for 10 minutes each to remove extra polymer. Finally, the sediment was re-suspended in Millipore water until use at room temperature.

2.1.3 Polymeric ((poly(lactic-*co*-glycolic) acid (PLGA)) NP

Nano-PLGA formulations were prepared by nano-precipitation technique with minor modifications by Dr. A.Uppal [99]. The chemicals: PLGA (poly(lactic-*co*-glycolic) acid) and PVA (Poly-vinyl alcohol) and HPLC grade acetone were purchased from Sigma. For particle synthesis 90 mg of PLGA was dissolved in 10 ml of HPLC grade acetone over a period of 3 h to get a uniform PLGA solution. This solution was drop wise added to 20 ml of aqueous solution containing 1.5% of PVA over a period of 10 min on a magnetic stir plate operated at 800 rpm. Within a few minutes, precipitation of nanoparticles was observed. This suspension was stirred at room temperature for 24 h to evaporate the acetone solvent completely. Larger aggregates and free PLGA/PVA polymers were removed by centrifugation at 5,000 rpm for 10 min. Then centrifuged at 18,000 rpm for 1 h and washed the sediment with water. These NPs were stable for more than six months at 10 degree centigrade.

2.1.4 Liposomes

Phosphatidylcholine (PC) was purchased from Sigma. Smaller unilamellar liposome of size ~30 nm, were prepared by injecting a 100ul ethanolic solution of phosphatidylcholine (PC, 20mg/ml) into 1.0 ml water/buffer at the required pH following the method as described in ref. [100]. Liposomes were prepared on the same day of the experiment.

Large unilamellar PC liposomes of size ~1µm were prepared using the method as described in ref. [101]. In this method a stock solution, containing 15.2mg PC dissolved in 10 ml chloroform, was first prepared. To a clean and dry 50 ml round bottom flask 1ml of this stock solution and 200 µl methanol was added. To this 7ml of distilled water/buffer was carefully added by the sides so that the two phases remain separate. Slowly the flask was attached to a rotary evaporator, at ~40 rpm under reduced pressure for ~two minutes, to evaporate the methanol (the flask was kept at temperature ~40 degree centigrade). After evaporation an opalescent fluid was obtained in the flask. To this added 3ml of distilled water/buffer. Thus ~1micrometer diameter liposomes were repared with 0.2mM lipid. These were stable for more than a week when stored at 10 degree centigrade.

2.2 Characterization of NPs

The morphology and structural properties of NPs were monitored by TEM imaging and their hydrodynamic radii were measured by light scattering methods such as dynamic light scattering and fluorescence correlation spectroscopy. To study the interaction of NPs with dyes, NPs were characterized for their surface charge, coatings as well as the functional groups, which were carried out by measuring their zeta potential and by studying their vibrational spectra by FTIR spectroscopy. The details are given below:

2.2.1 Transmission Electron Microscopy

The TEM imaging of SiNPs and gold nanorods was done using model CM200 from Phillips, operating at 200kV with 2.5Å point-to-point resolution. Samples for TEM were

prepared by dipping the carbon coated copper grid in the nanoparticles solution and evaporating in the dark. This process was repeated a few times to get sufficient number of nanoparticles in the field of view. The TEM images of SiNPs and gold nanorods, of two different aspect ratios, are shown in Fig. 2.2 and Fig. 2.4 respectively.

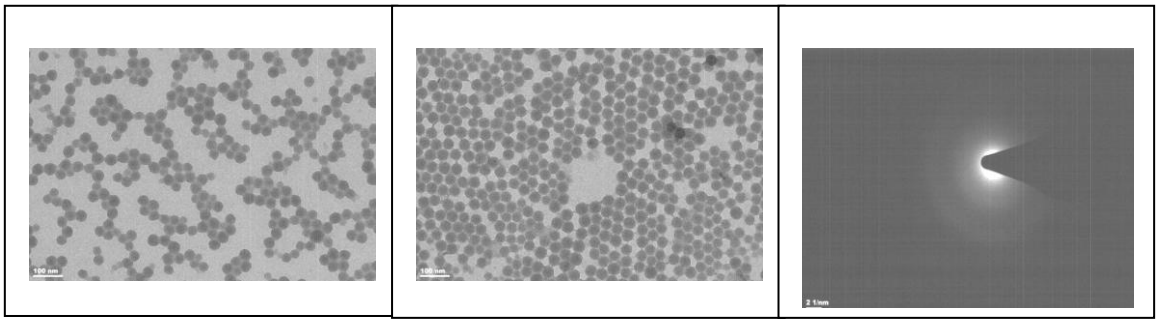

SiNP-VA , Size~30±5 nm SiNP-V, Size~30±2 nm SAED

Figure 2.2 *TEM pictures of SiNPs and their typical electron diffraction pattern*

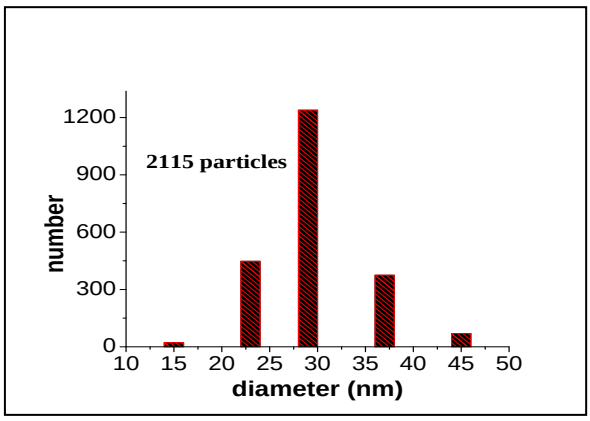

Figure 2.3 *Size distribution of SiNPs showing mean size ~30 nm*

Selected area electron diffraction (SAED) pattern indicating their amorphous and crystalline nature is also shown in the figures. SAED pattern in Fig.2.2 shows a series of rings indicating the amorphous nature of SiNPs whereas a pattern of dots, in the Fig.2.4, indicate that the gold nanorods are single crystal. The analysis of the size distribution of SiNPs and gold nanorods is shown in Fig. 2.3 and Fig. 2.5 respectively. For this more than 1000 particles of each category were analyzed to get good statistics.

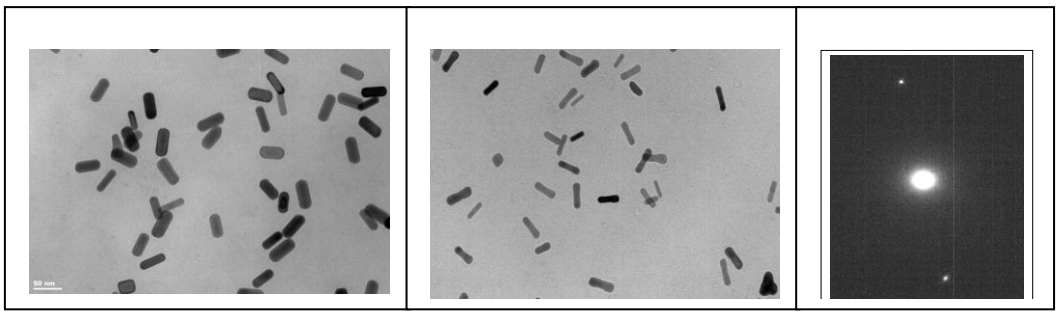

AR 2.5, length~50 nm AR 3.8, length~38 nm SAED

Figure 2.4 *TEM Pictures of gold nanorods and their SAED*

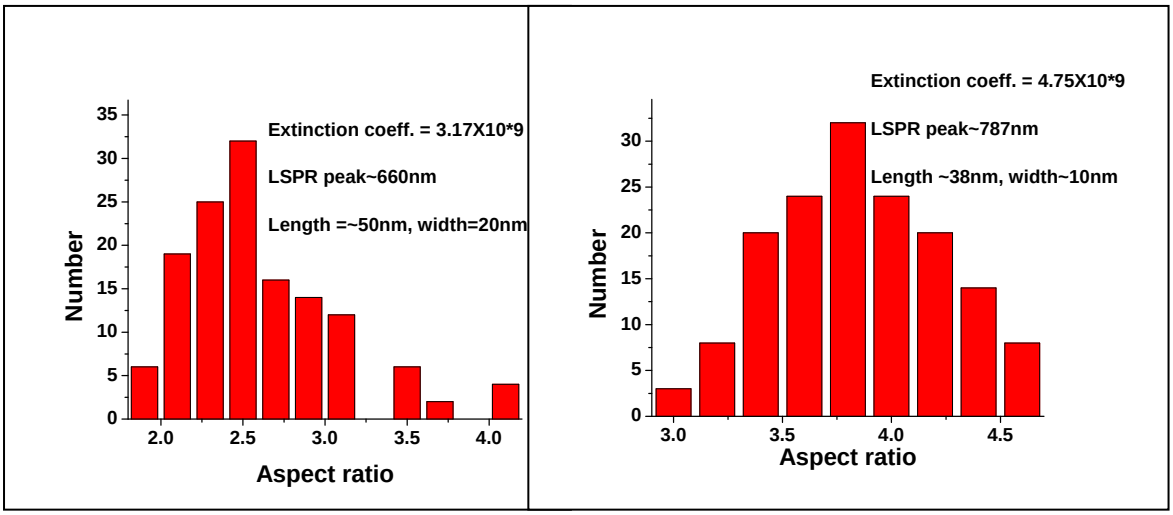

Figure 2.5 *Size distribution of AuNRs showing rods with aspect ratios, left (2.5) and right (3.8)*

The extinction coefficients of the prepared gold nanorods, was estimated using the methodology described in ref. [103], where they have shown a linear variation of extinction coefficient with respect to the aspect ratio as well as the L-SP resonance peak. The aspect ratio of our rods was obtained from TEM image analysis as shown in Fig. 2.4 and 2.5 and the L-SP maxima position was obtained from their extinction spectra using the UV-visible spectrophotometer. For the experiments conducted using these nanorods, the molar ratio of the differently coated rods and the dye molecules were kept same.

2.2.2 Hydrodynamic radius measurement

Dynamic light scattering:

The diffusion time of the particles in the probe volume is proportional to their hydrodynamic radii (When a charged particle is suspended in a liquid, counter ions are attracted at higher concentration closer to its surface forming a thin layer. This forms an electrical double layer. The particle and this double layer of ions adsorbed on to its surface move together as the kinetic unit or hydrodynamic unit as the particle diffuses through the solvent. The radius of these particles is called hydrodynamic radius). The hydrodynamic radius of the non-fluorescent particles suspended in aqueous medium can be easily measured by dynamic light scattering (DLS) methods.

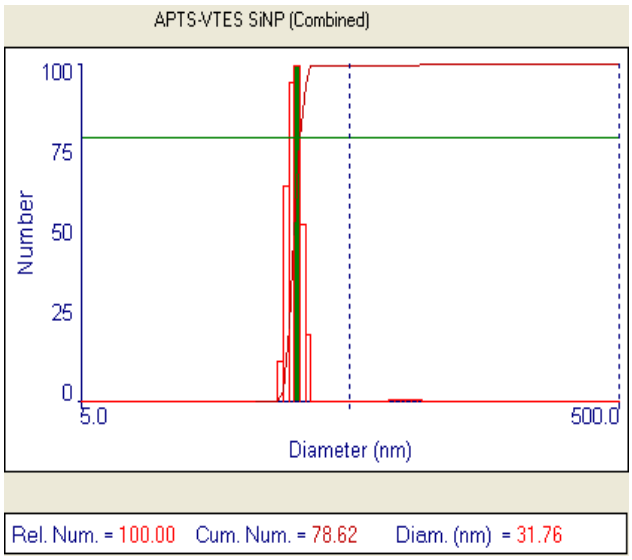

Figure 2.6 *Showing the mean size (~31.76 nm) and distribution of SiNP-VA as measured by DLS. The polydispersity is ~16%.*

We measured it using particle size analyzer 90Plus, from Brookhaven. It can measure the size of particles in the range from ~1 nm to 6 µm. It uses a 35 mW diode laser as the light source and the scattered signal is collected at 90°. The sample volume required is ~3ml. For correct measurements, the particles are diluted in a suitable solvent to single scattering regime. With this system an average diameter of the particles and

along with the distribution width (polydispersity) is obtained. Fig. 2.6 shows the size of SiNP as measured using 90Plus instrument. It is pertinent to note that the hydrodynamic size is slightly higher than that shown by TEM imaging. This is because of the counter ion layers attached to the charged particles which move together with the particle in the suspension as the hydrodynamic unit.

Fluorescence Correlation Spectroscopy:

Fluorescence correlation spectroscopy (FCS) is similar to DLS spectroscopy where the hydrodynamic radius of the particles is measured by monitoring their fluorescence. While both FCS and DLS use a small sample volume to noninvasively probe the concentration fluctuations, it is the enhanced sensitivity of fluorescence to conformational, environmental, and chemical changes in a system that allows FCS to be more useful in these scenarios than tracking scattered light [104, 105].

The FCS experiments were performed on a FCS spectrometer built around an Olympus IX71 inverted microscope. The excitation laser (SDL 532LN002T, 15 mW, 532 nm, Frequency doubled Nd: YVO4, Shanghai Dream Laser, Shanghai, China) was coupled through the rear port of the microscope. The collimated laser light is passed through a dichroic filter, and focused on the sample with an Olympus 60x water immersion objective (N.A. = 1.2). The fluorescence emission from sample was collected using the same objective and reflected from the dichroic filter and passed through a long pass filter to eliminate the excitation light before detection using a single photon counting APD (SPCM-AQRH-13-FC, Perkin Elmer, Canada). The autocorrelation function of detected fluorescence intensity fluctuation was calculated using FLEX99OEM-12D correlator card.

2.2.3 Zeta potential measurements

Zeta potential is a measure of the stability of colloidal particles and is measured from the electrophoretic mobility of the kinetic unit under an applied field. The electrophoretic

mobility is defined as the electrophoretic velocity divided by the strength of the electric field which depends on the applied voltage and the electrode geometry.

$$V=\mu_e E$$

Where V is the velocity, μ_e is the mobility and E is the applied electric field. From the measured velocity the mobility and zeta potential are calculated typically (under certain approximations) as follows:

$\mu_e=(2e\zeta)/(3\eta)$, where ζ is the zeta potential, η is the viscosity.

To measure zeta potential, electric field is applied to the nanoparticle dispersion in a liquid. As these are charged particles, they will move to the respective oppositely charged electrodes. The direction of their movement indicates the kind of charge on them and the velocity with which they move is proportional to the magnitude of the charge. In the present thesis, the system used for measurement of Zeta potential is 'ZetaPlus' from Brookhaven Instruments Corporation. It can measure zeta potential of nanoparticles from -150 to 150mV, size range from 10 nm to 30 µm with accuracy ±2%.

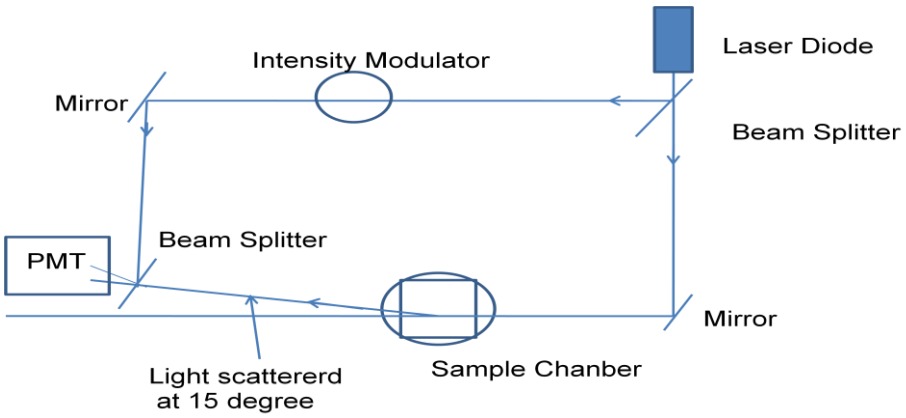

Figure 2.7 *Optical heterodyne used for zeta potential measurement.*

In the Zeta plus system, a laser beam is passed through the sample placed in a cell which has two electrodes to provide the electric field as shown in Fig.2.7. As the particles are moving in the electric field, light which is scattered by the particles is Doppler shifted.

This shift ~100Hz is measured by making use of the principle of optical heterodyning. In this a portion of the beam is split off and then recombined with the scattered beam after it is modulated at 250 Hz. In the absence of field, the power of the signal from the detector would have sharp peak at 250 Hz. When field is applied, there is a shift in the frequency due to the Doppler velocity. If the resultant frequency is less than 250Hz the particles are negatively charged and vice versa. From this Doppler frequency shift, which is proportional to electrophoretic velocity, mobility can be measured. Zeta potential depends upon charge and solution condition such as pH in water, electrolyte concentration etc. and therefore these are needed to be specified. The square of zeta potential is proportional to force of repulsion between two charged particles. As a general experience for zeta potential > +25mV and < -25mV, the repulsion is considered to be sufficient and the dispersion is likely to be stable. Without steric hindrance, to keep particles apart, as the zeta potential approaches zero, dispersion is likely to be unstable. The Zeta potential values of NPs are given in respective chapters.

2.2.4 FTIR spectroscopy

Fourier transform infra-red (FTIR) spectrometer provides information of various vibrational transitions. The principle of FTIR spectrometer is different from that of normal dispersive spectrometer which separates the optical frequencies spatially. FTIR spectrometer modulates different frequencies of the light and uses Fourier Transform to separate them. The heart of the FTIR spectrometer is a Michelson interferometer, which in simplest form consists of a fixed mirror, a moving mirror and a beam splitter. The light from the infrared source, a glowbar, enters the interferometer and is divided into two equal beams by a beam splitter. One beam is reflected towards a fixed mirror, which reflects it back towards the beam splitter. The other beam is transmitted towards the moving mirror, which also reflects it back towards the beam splitter. The moving mirror introduces a continuously changing path difference between the two beams. As the

moving mirror is scanned, the two returned beams interfere with different phases. This creates intensity variations. At a given path difference, the interference is constructive for some frequencies and destructive for others. As the optical path difference is continuously changing, the various frequencies present in the beam are modulated at different times as the mirror is moved. After leaving the interferometer, the modulated light passes through the sample.

If the sample contains non symmetrical molecules, these will absorb IR at specific frequencies. The remaining light then reaches the detector which converts it into an electrical signal. The plot of the interference intensity, called an interferogram, as the function of the position of the mirror is related to the intensity of light as a function of frequency by mathematical relation called Fourier transform. Performing a Fourier transform, with the help of computer program, on the interferogram yields a raw spectrum, which is a graph of the light intensity at the detector versus the optical frequency. This type of the spectrum contains information about the sample as well as the whole instrument response which include the source, all the optical components, ambient air, as well as contamination in the optical path. To extract the sample information from this raw data, a reference spectrum is acquired under the same ambient condition without the sample. The data acquisition software uses the reference and the raw data to normalize the sample spectrum with the instrument response. The FTIR spectrometer used to characterize the NPs was FT-IR, FTLA 2000 MB 104, from ABB Bomem. The spectra were taken at resolution of 1 cm-1. To get good signal to noise ratio ~ 40 scans per sample were taken (depending upon the sample).

FTIR spectra of SiNP-V, SiNP-VA, along with the silica precursors VTES and APTS and the surfactant AOT are shown in Fig. 2.8. In the spectra of SiNP-V and SiNP-VA, the abscence of the dominant peak of asymmetrical sulphonate stretch peaks of AOT at 1248 cm^{-1} indicates the removal of surfactant AOT from the SiNP aqueous suspension after dialysis. The strong peaks at ~1043 cm^{-1} and ~1130 cm^{-1} are assigned to Si-O-Si

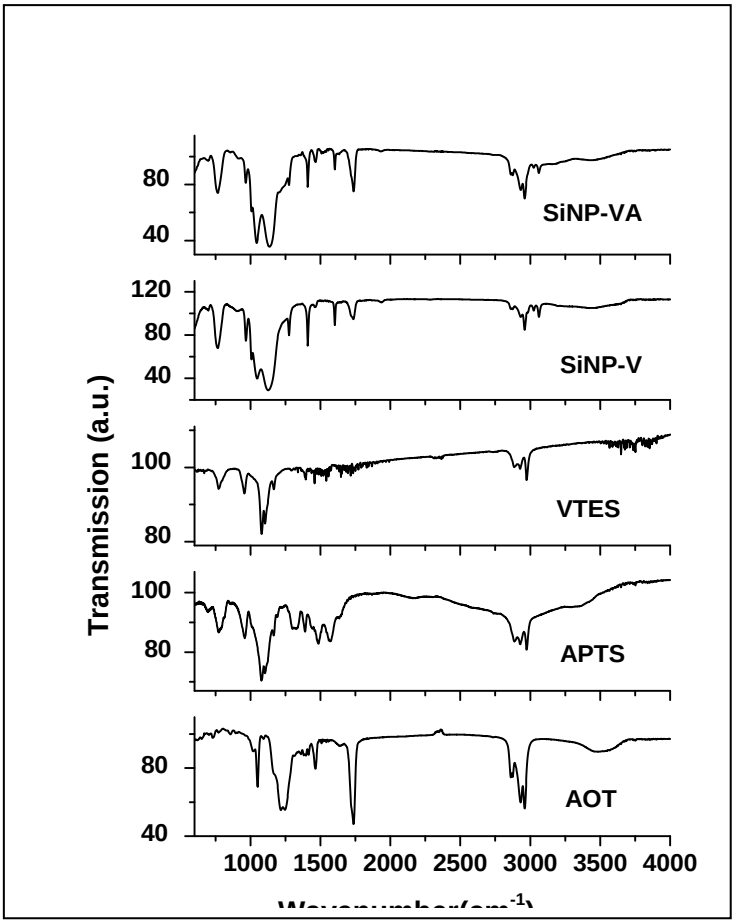

Figure 2.8 *FTIR spectra of different components of ORMOSIL NP.*

stretch, which indicates polymerization and are absent in the APTS and VTES whereas the peaks at 1104 and 1081 cm-^{1}, are assigned to Si–O–C in VTES and APTS, which are absent in the nanoparticles [97]. The hump at the ~3400 cm^{-1} and 1640 cm^{-1} in both APTS and SiNP-VA denotes the presence of weak amine N-H stretch and bend band respectively.

The coatings on the gold nanorods were also confirmed by FTIR spectroscopy. In Fig.2.9, the FTIR spectra of coated gold rods along with the corresponding coating materials: CTAB, PSS, PAH and PDDAC are shown in graphs A, B, C and D respectively. The presence of characteristic IR peaks of the polymers (black) on the coated rods (in red), with few cm^{-1} shifts, confirms the coating. Graph A shows the

spectra of CTAB coated rods where the peaks at ~2915 cm^{-1} and ~2850 cm^{-1} correspond to CH asymmetric and symmetric stretching respectively.

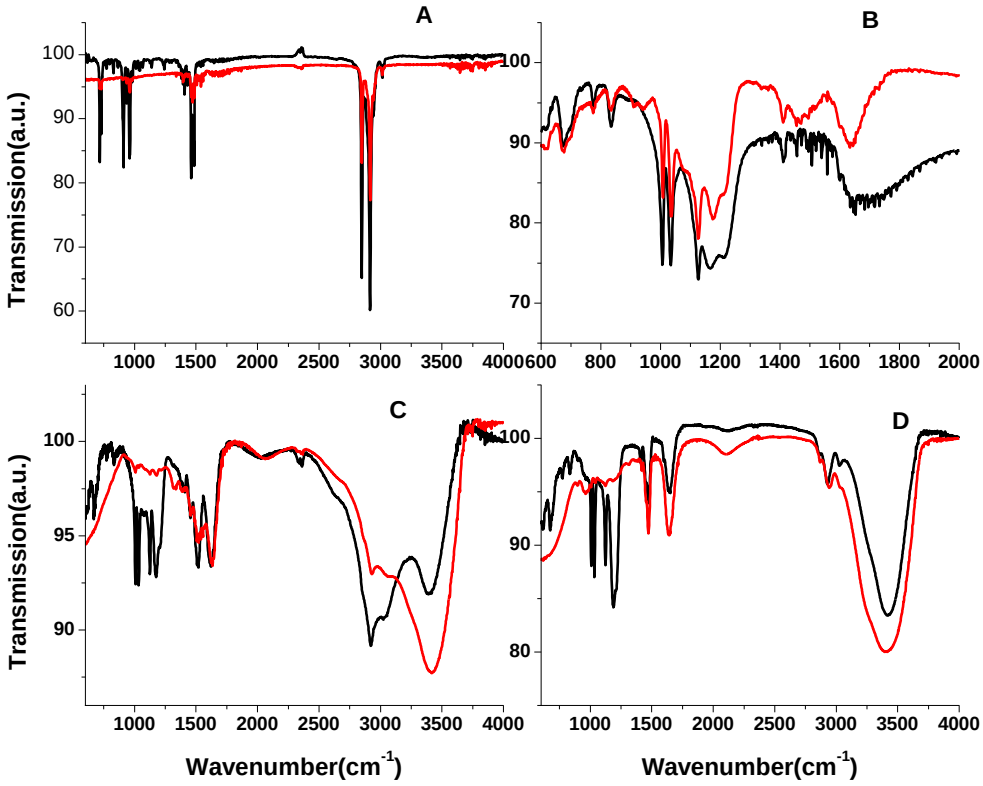

Figure 2.9 *FTIR spectra of four coated gold rods (in red), coated with A)CTAB, B)PSS, C)PAH and D)PDDAC along with the respective polymers (black)*

In case of PSS coated rods, graph B, the presence of sulphonate S=O asymmetric stretch at ~1215 cm^{-1} and ~1175 cm^{-1} and symmetric stretch frequencies at 1035 cm^{-1} confirm PSS coating. In graph C, the PAH coating on the rods is confirmed by the presence of the NH absorption at ~3400cm^{-1}, the C-C stretch at 1460cm^{-1} and NH_2 scissoring at ~1622 cm^{-1}. Similarly, in graph D, the presence of NH absorption at ~3400 cm^{-1}, ethylene at 1630 cm^{-1} and CH_3 bend at 1471 cm^{-1} in PDDAC coated rods as well as in polymer confirm coating.

2.3 UV-visible spectroscopy

2.3.1 Absorption spectroscopy

The steady state absorption spectra were measured using a UV–VIS absorption spectrometer model Cintra 20 (GBC Scientific Equipments Ltd.). It is a dual beam direct ratio recording system having Czerny-Turner style monochromators with holographic grating and variable slit widths and the detector is a photomultiplier tube. Automatic lamp peaking and wavelength calibration is done on power up. The excitation sources are 35 W tungsten–halogen lamp and 30 W deuterium lamp which change automatically at selected wavelength. Wavelength range is 190-900 nm with spectral band pass from 0.2 nm to 5 nm variable in steps of 0.1 nm with wavelength accuracy ±0.2 nm. Photometric linearity is better than 1% up to absorbance 3. In our studies, all the measurements were done at the resolution of 1 nm.

2.3.2 Emission spectroscopy

The steady state emission measurements were carried out using Spex Fluorolog 2 fluorimeter. It has a 450 W Xenon lamp as the excitation source. The excitation light is passed through a 20 cm monochromator and is focused on the sample placed in the sample chamber at spot size ~2 mm by 6 mm. For most of the samples, the emission was collected at 90 degree (& at 15 degree, front face, for optically dense samples). The emitted fluorescence after passing through a double monochromator (each 20cm focal length) was collected by PMT (Hamamatsu R955) which is sensitive from 250 to 850 nm. With each slit as 1mm, the system resolution was 4 nm. All the measurements were done at this resolution.

2.3.3 Fluorescence lifetime measurement

The time resolved fluorescence measurements were done using time correlated single photon counting (TCSPC) system. This method of fluorescence decay time measurement is based on the concept that after an excitation event, the temporal probability distribution

of emission of a single photon yields the actual intensity against time distribution of all the emitted photons. In the experiment this probability distribution is constructed by sampling a single photon emission, following a large number of excitation events.

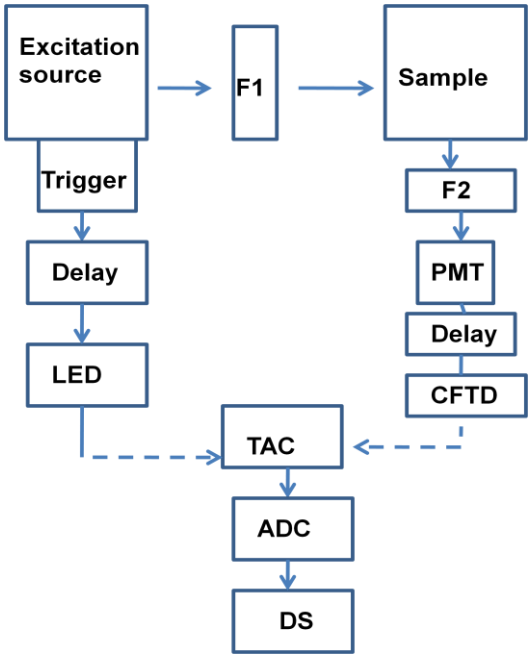

Figure 2.10 *Block diagram representing the concept of time correlated single photon counting. Here Excitation source is a pulsed light source, F1 and F2 are the filters/monochromators, PMT is a fast photomultiplier tube, 'Delay' are the delay lines to adjust the start and stop pulse times. LED is the leading edge timing discriminator, CFTD is the constant fraction timing discriminator, TAC is time to amplitude convertor, DS is the data storage device (computer). Recreated from ref. [106].*

Fig.2.10 shows the block diagram of a TCSPC set-up. Here a trigger pulse generates an electrical pulse at a time which is exactly correlated with the time of generation of the pulse of the excitation source (a fast optical pulse). This pulse is routed through a discriminator to the start input of the time to amplitude convertor, (TAC) which initiates charging of a capacitor. In the mean time the optical pulse excites the sample, which subsequently fluoresces. The intensity of the fluorescence at the photomultiplier tube is so adjusted that at the most one photon is detected for each exciting event. The electrical signal generated due to this photon stops the charging ramp in the TAC, and

gives out a pulse, the amplitude of which is proportional to the charge in the capacitor and hence to the time difference between START and STOP pulses.

The TAC output pulse is given a numerical value, depending upon its amplitude, in the analogue-to-digital converter and a count is stored in the data storage device against an address corresponding to that number. This excitation and storage process is repeated until the histogram of the number of counts against address number in the storage device represents the decay curve of the sample to a required precision. For deconvolution the temporal profile of the exciting pulse is also collected in the similar way by replacing the sample by light scatterer [106].

The emission lifetimes of the fluorophores were recorded by using a TCSPC module Lifespec-RED from Edinburgh Instruments. The excitation source was either a 40 ps Pico-Quant laser diode (LDH-P-C-400) at 406 nm (operated at 2.5 MHz repetition rate, average power <1 mW) or the second harmonic output of the tunable femto second laser (Coherent Verdi pumped by Mira) having pulses of ~100 fs duration. Coherent model 9200 pulse picker was used to select pulses at 3.8 MHz repetition rate. The fluorescence was collected at 90 degree. Proper high pass and low pass filters were used to avoid the excitation pulse scattered photons to enter the collection lens. The detector was a thermoelectric cooled Hamamatsu photomultiplier tube (H7422) or microchannel plate PMT (R3809U-50). The instrument response function (IRF) along with PMT was ~200ps whereas with MCP PMT was ~50ps. The fluorescence decays were deconvoluted from the IRF using the iterative software based on global least squares analysis algorithm provided by the manufacturer. The goodness of the fit was judged by the reduced chi-square values and visual inspection of the plots of weighted residuals. For time resolved anisotropy calculations the anisotropy was first constructed from the parallel and perpendicular polarized traces and then deconvoluted from the IRF using the above mentioned algorithm.

2.4 MTT Assay, to determine the cell survival

This is a quantitative colorimetric assay proposed by Mosmann in 1983, for determining mammalian cell survival and cell proliferation [102]. The assay is dependent on the reduction of the tetrazolium salt MTT (3-(4,5-dimethylthiazol-2-yl)-2,5-diphenyltetrazolium bromide) by the mitochondrial dehydrogenase generated from viable cells which leads to the formation of a blue formazan product. The assay measures cell respiration and the amount of formazan produced is proportional to the number of living cells present in culture. In our experiments, 100 µl of medium containing MTT (10µl, 5 mg/ml) was added to each well containing the cells, in the 96 well standard microplate, after the treatment followed by incubation for 4 h. The culture medium was then removed and the formazan crystals formed were dissolved in isopropanol-HCl (0.4 N) solvent mixture. The optical density of the dissolved formazan was measured at 570 nm using a microplate reader (Power Wave 340, Biotech instruments, USA).

2.5 Molarity calculation of the NPs

To maintain the desired dye to NP ratio in the experiments, the molarity of ORMOSIL NPs and gold nanorods was calculated as follows:

For calculating the molarity of ORMOSIL NPs, first the average size of SiNP was measured by either TEM or by light scattering methods which was ~30 nm. The dry weight of 1ml colloid was obtained as ~5 mg. The density of SiNP was taken as ~1.9 g/cc. For the volume of 1NP = $4/3\ \pi\ r^3$, keeping r =15 nm, the average mass of 1 NP was obtained as $26{,}847 \times 10^{-21}$ gm. Hence, the morality of the prepared SiNP was obtained ~300 nM. The molarity of gold nanorods was calculated by first knowing their aspect ratio. This was done by measuring dimensions (length and width) of a sufficient number (~1000) of rods (of each type) so as to generate the histogram as shown in Fig.2.5. Rest of the details are discussed in section 2.2.1.

2.6 Conclusion

The NPs were synthesized, following wet chemical methods and characterized using TEM, light-scattering methods, Zeta potential measurements and FTIR spectroscopy for their size, surface properties and stability. These were stored as colloidal suspensions and used for the studies described in the following chapters.